

Reprint 1120

An Assessment on the Transportation of Artificial Radionuclides  
Arising from the Fukushima Nuclear Accident to Hong Kong

W.M. Ma, S.M. Olivia Lee, W.H. Leung

Delia Arnold<sup>\*</sup>, Gerhard Wotawa<sup>\*</sup> & Christian Maurer<sup>\*</sup>

Presented in the IAEA International Expert's Meeting on  
Radiation Protection after the Fukushima Daiichi Accident,  
Vienna, Austria 17 February 2014

<sup>\*</sup>Central Institute of Meteorology and Geodynamics, Austria

# **An assessment on the transportation of artificial radionuclides arising from the Fukushima Nuclear Accident to Hong Kong**

W.M. Ma<sup>a</sup>, Olivia S.M. Lee<sup>a</sup>, W.H. Leung<sup>a</sup>,  
Delia Arnold<sup>b</sup>, Gerhard Wotawa<sup>b</sup> and Christian Maurer<sup>b</sup>

<sup>a</sup>Hong Kong Observatory

<sup>b</sup>Central Institute of Meteorology and Geodynamics, Austria

## ***Abstract***

*Shortly after the Fukushima nuclear accident in March 2011, the Hong Kong Observatory stepped up its environmental radiation monitoring programme. Minute amounts of <sup>131</sup>I and <sup>137</sup>Cs were detected in a number of environmental air samples taken in Hong Kong, some 3,000 kilometres southwest of the Fukushima Daiichi Nuclear Power Plant, in late March and April 2011.*

*This paper discusses the dispersion pathway of the artificial radionuclides with reference to the meteorological conditions in East Asia and the Pacific Ocean. The HYSPLIT single particle dispersion model is employed to study the trajectories of the radionuclides in the atmosphere. Furthermore, the Lagrangian particle dispersion model FLEXPART is also used to simulate the spread of the radioactive release, with source term estimated by Chino et al. (2011) and modified by Terada et al. (2012). Model simulations are compared with the radiation monitoring results in the region. The assessment is that the probable pathway in the transport of artificial radionuclides from eastern Japan to Hong Kong could be attributed to the prevailing northeast monsoon, with the likelihood that the first arrival might have taken a tortuous route through eastern Russia and mainland China.*

## **1. Introduction**

### **1.1 Environmental Radiation Monitoring in Hong Kong**

The Hong Kong Observatory is responsible for environmental radiation monitoring in Hong Kong. The work began in 1961 when the Observatory started to measure beta radioactivity of air particulates, total deposition and rain-water at King's Park meteorological station (Hong Kong Observatory, 1997). Around the same time, the Observatory started to participate in international

programmes on environmental radiation monitoring – namely a joint programme "World Survey of Isotope Concentration in Precipitation" organized by the International Atomic Energy Agency (IAEA) and the World Meteorological Organization; and a co-operative programme with the Atomic Energy Research Establishment (AERE), United Kingdom.

After the nuclear reactor accident at Chernobyl in 1986, the Observatory stepped up atmospheric sampling in Hong Kong. Radiation measurement results indicated that an insignificant but nonetheless measurable amount of fallout was detected in Hong Kong (Lee *et al.*, 1991).

In 1987, in response to the planned establishment of a nuclear power station at Daya Bay in Guangdong, China, about 50 kilometres away from the city centre of Hong Kong, a comprehensive Environmental Radiation Monitoring Programme (ERMP) was implemented. The first phase of ERMP, known as the Background Radiation Monitoring Programme, was conducted in the 5-year period from 1987 to 1991 to establish the baseline radiation levels in Hong Kong before the operation of the nuclear power station in 1994 (Hong Kong Observatory, 1992). The second phase of ERMP, launched in 1992, is an on-going programme and focuses on finding out the changes, if any, in the amount of artificial radionuclides in the environment, including air, rain, soil, sea water and foodstuff, before and after the establishment of the nuclear power stations at Daya Bay.

## **1.2 Fukushima Nuclear Accident**

On 11 March 2011, a severe earthquake of magnitude 9.0 rocked the east coast of Honshu, Japan. The tsunami generated by the earthquake triggered a beyond-design-basis accident at the Fukushima Daiichi Nuclear Power Plant, ultimately declared as a Level 7 accident ("Major Accident") according to the International Nuclear and Radiological Event Scale (National Diet of Japan, 2012).

The Fukushima Daiichi Nuclear Power Plant consists of six reactor units. As indicated in a number of reports (e.g. IAEA, 2011; National Diet of Japan, 2012), when the earthquake occurred at 14:46 local time on 11 March, the emergency shut-down features of Units 1, 2 and 3 did immediately go into operation. It was the tsunami generated by the earthquake, with peak waves at 15:37 local time, that totally destroyed the emergency diesel generators, the sea water cooling pumps, the electric wiring system and the DC power supply for Units 1, 2 and 4, resulting in loss of all power except for an external supply to

Unit 6 from an air-cooled emergency diesel generator. With the loss of power, the cooling systems of the reactors simply did not function. Hydrogen explosion occurred at Units 1, 3 and 4 and there was reactor core damage at Units 1, 2 and 3 from 11 to 14 March, with massive discharge of radioactive materials into the environment on 15 March.

### 1.3 Enhanced Environmental Radiation Monitoring in Hong Kong

Even though Hong Kong is about 3,000 kilometers southwest of the Fukushima Daiichi Nuclear Power Plant, environmental radiation monitoring in Hong Kong was enhanced shortly after the accident. In particular, sampling of airborne particulates was stepped up and additional samples were collected daily at designated monitoring stations, in addition to the routine weekly and monthly samples. A map showing the various enhanced environmental radiation monitoring activities carried out between March and May 2011 in Hong Kong is given in Figure 1.

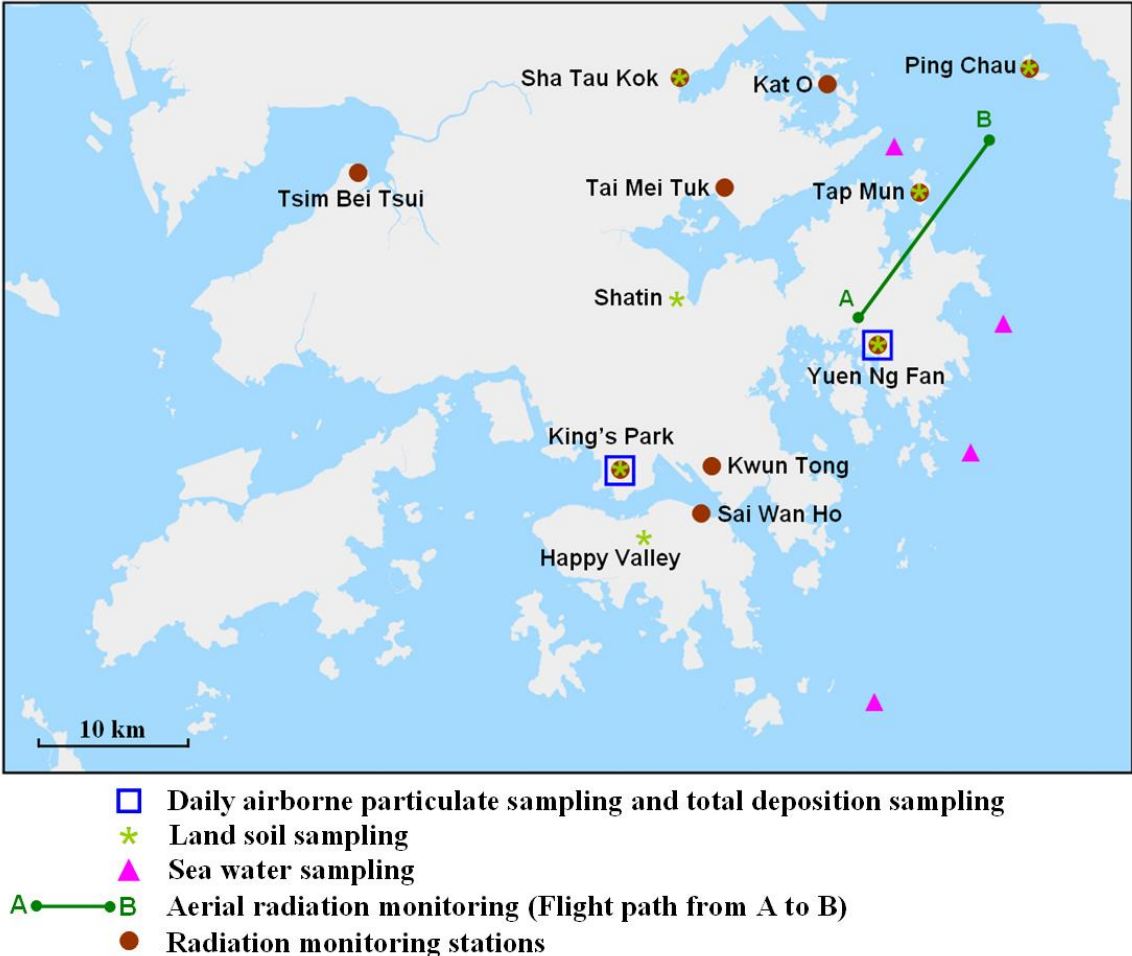


Figure 1 Locations of enhanced radiation monitoring of airborne particulate, total deposition, land soil and sea water, as well as aerial radiation monitoring in Hong Kong from March to May 2011. Real-time ambient gamma radiation levels are measured routinely at ten radiation monitoring stations.

Eventually, minute amounts of  $^{131}\text{I}$  and  $^{137}\text{Cs}$  were detected from some of the daily air samples collected through high volume air samplers in late March and early April. Minute amount of  $^{134}\text{Cs}$  was also detected in the routine monthly air sample for April 2011. For other artificial radionuclides, including Ru-106, Sr-90 and Pu-239, measurement results for samples taken between March and May 2011 from various radiation monitoring activities indicated that they were either below the Minimum Detectable Activity<sup>1</sup> (MDA) or within baseline levels. Detailed measurement results from the routine and enhanced monitoring can be found in Lee *et al.* (2012).

Table 1 and Figure 2 summarize the measurement results from the daily airborne samples taken at King's Park. It is noted that  $^{131}\text{I}$  was first detected from the sample taken on 27 March. Activity levels in the samples in the next three days increased gradually to a peak value of  $0.83 \text{ mBq/m}^3$  on 30 March. After a lull period between 2 and 5 April,  $^{131}\text{I}$  was again detected from 6 to 14 April, except for the daily sample collected on 12 April. Furthermore,  $^{137}\text{Cs}$  was present in the daily samples collected at King's Park on 9 and 13 April. Despite the presence of minute amount of  $^{131}\text{I}$  and  $^{137}\text{Cs}$ , there was no detectable change in the ambient gamma dose rates at all radiation monitoring stations in Hong Kong.

Table 1 Activity of  $^{131}\text{I}$  and  $^{137}\text{Cs}$  in King's Park Daily Airborne Particulate Samples

Sampling Date <sup>2</sup>	Activity of $^{131}\text{I}$ <sup>2</sup> [MDA: 0.1-0.2] (mBq/m <sup>3</sup> )	Activity of $^{137}\text{Cs}$ <sup>3</sup> [MDA: 0.1-0.2] (mBq/m <sup>3</sup> )
16 March to 26 March 2011	Below MDA	Below MDA
27 March 2011	$0.06 \pm 0.06$	Below MDA
28 March 2011	$0.19 \pm 0.07$	Below MDA
29 March 2011	$0.30 \pm 0.07$	Below MDA
30 March 2011	$0.83 \pm 0.12$	Below MDA
31 March 2011	$0.65 \pm 0.10$	Below MDA
1 April 2011	$0.36 \pm 0.09$	Below MDA
2 April to 5 April 2011	Below MDA	Below MDA
6 April 2011	$0.26 \pm 0.06$	Below MDA
7 April 2011	$0.32 \pm 0.07$	Below MDA
8 April 2011	$0.06 \pm 0.07$	Below MDA
9 April 2011	$0.17 \pm 0.08$	$0.07 \pm 0.02$
10 April 2011	$0.14 \pm 0.06$	Below MDA
11 April 2011	$0.17 \pm 0.08$	Below MDA
12 April 2011	Below MDA	Below MDA
13 April 2011	$0.15 \pm 0.05$	$0.03 \pm 0.03$
14 April 2011	$0.07 \pm 0.05$	Below MDA
15 April to 25 May 2011	Below MDA	Below MDA

<sup>1</sup> MDA in this context are values under typical measurement conditions. Under some specific measurement conditions, activity lower than the typical MDA can sometimes be measured.

<sup>2</sup> Results of radionuclide analyses are reported as " $xx \pm yy$ ", where xx is the activity level and yy is the counting uncertainty at the 95% confidence level.

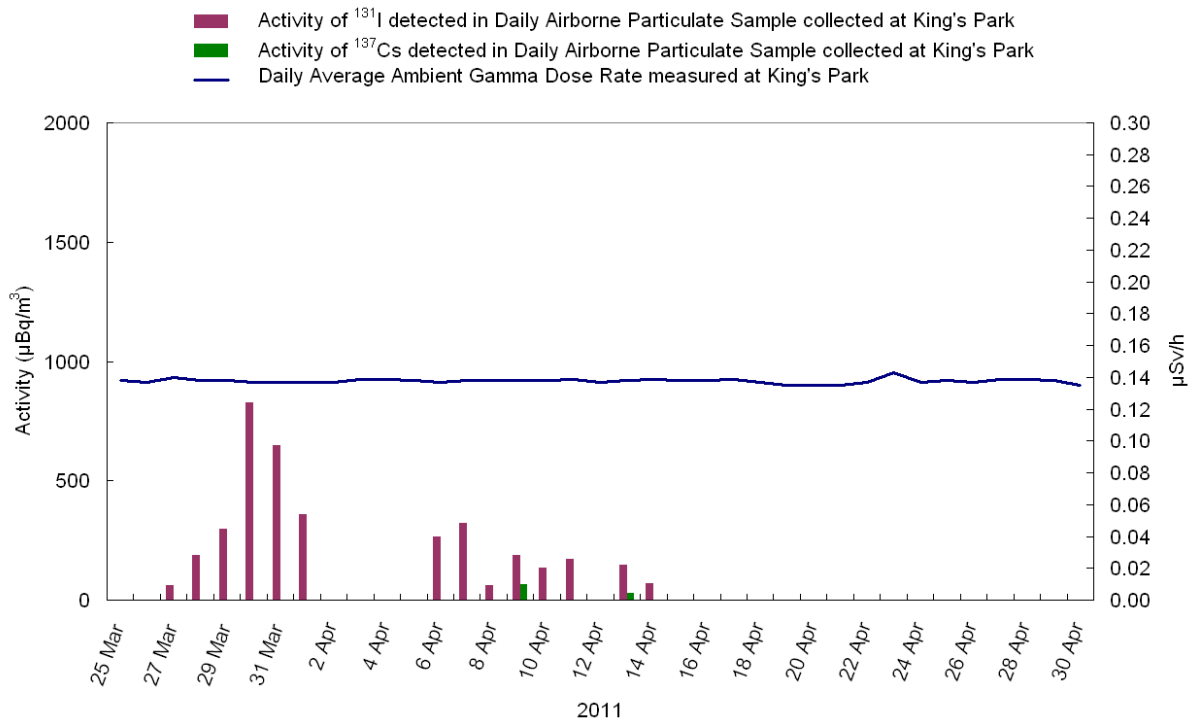


Figure 2 Daily average ambient gamma dose rates measured and activity of  $^{131}\text{I}$  and  $^{137}\text{Cs}$  in daily airborne particulate samples collected at King's Park from 25 March to 30 April 2011.

## 2. Transportation of Artificial Radionuclides from Fukushima to Hong Kong

To examine how the artificial radionuclides were transported from Fukushima to Hong Kong, the synoptic patterns over East Asia and the Pacific Ocean, as well as radiation monitoring results reported over the region were analyzed. The HYbrid Single-Particle Lagrangian Integrated Trajectory (HYSPLIT) model (Draxler and Hess, 1998; Draxler and Rolph, 2014) was also employed to simulate the forward trajectories of the releases in the first few days and the backward trajectories for arrival at Hong Kong in late March 2011.

With reference to the IAEA EMERCON messages and as pointed out in other studies (Stohl *et al.*, 2011), the heights of releases were estimated to be below 1,000 m. As such, we focused on the possible trajectories of radionuclides released at altitudes of 50, 500 and 1,000 m.

A number of HYSPLIT simulations were carried out, initialized between 12 and 15 March 2011, with trajectories originating from the Fukushima Daiichi nuclear power plant for assessing the initial transport of the radioactive substances. For all HYSPLIT simulations in this study, meteorological analysis data are from National Centers for Environmental Prediction (NCEP)'s Global

Data Assimilation System at 1° x 1° spatial resolution and 3-hour temporal resolution.

Figure 3 shows the HYSPLIT simulation initialized at 10 UTC 12 March 2011, a few hours after the first reported explosion at the Daiichi Unit 1 reactor. As pointed out in other studies (e.g. Chino *et al.* 2011, Sothl *et al.*, 2011; Masson *et al.*, 2011), at the initial stage, radioactive substances released into the atmosphere over eastern Japan generally followed the westerlies and spread eastwards across the Pacific. The simulation results in Figure 3 indicated that while the trajectories from altitudes of 500 and 1,000 m continued to move towards North America, releases originating at the height of 50 m appeared to undergo a looping motion in the vicinity of the Kamchatka Peninsula and travelled at an altitude of around 3,000 m on 18 March. Similar results were also obtained by Leon *et al.* (2011) using HYSPLIT for simulating the initial transport of radioactive substances from Fukushima.

Figure 4 shows the HYSPLIT simulations initialized between 13 and 15 March at 00 UTC and 12 UTC daily, and at release heights of 50, 500 and 1,000 m. The results also indicated that most of the trajectories pointed mainly eastward by following the mid-level westerlies across the Pacific, while the others moved to the Bering Sea and its surroundings at around the same period, at altitudes of 3,000 m or above.

Corresponding roughly to an altitude of 3,000 m, the 700-hPa wind and streamline analysis charts on 12 and 18 March showed that the depression over the Bering Sea intensified (Figure 5(a)). Development of this cyclonic circulation explains the looping motion of air masses in the vicinity of Kamchatka Peninsula as revealed by the above HYSPLIT simulation.

Based on the above HYSPLIT assessment and the synoptic evolution, it is reasonable to believe that some of the radioactive substances would linger around Kamchatka Peninsula and Bering Sea around 18 March and the following couple of days.

From 19 to 21 March, the cyclonic vortex drifted westward and lingered over the sea area west of the Kamchatka Peninsula with its circulation extending to cover Heilongjiang in northeastern China (Figure 5(b)). Under the influence of this cyclonic flow, some of the radioactive substances near the Kamchatka Peninsula might have moved in an anti-clockwise direction towards northeastern China along the western flank of the cyclonic circulation.

NOAA HYSPLIT MODEL  
 Forward trajectories starting at 1000 UTC 12 Mar 11  
 GDAS Meteorological Data

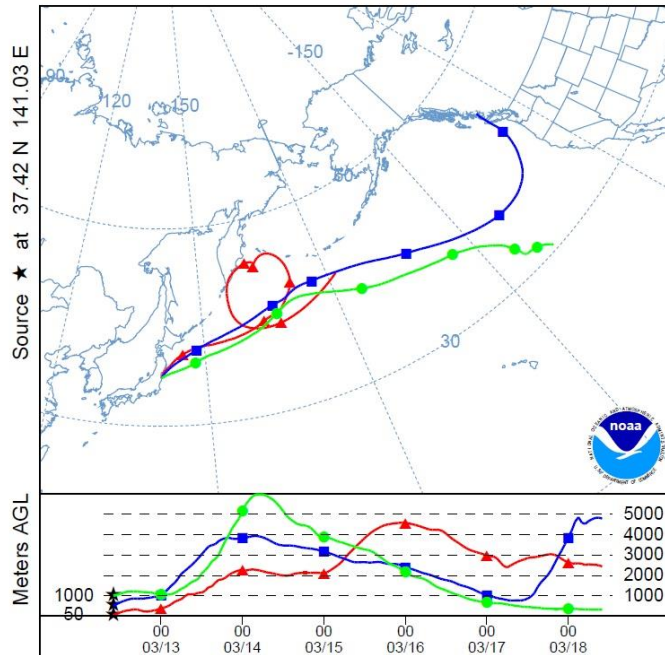


Figure 3 Trajectories of air masses released at heights of 50 m (red), 500 m (blue) and 1,000 m (green) from the Fukushima Daiichi nuclear power plant originating at 10 UTC 12 March 2011 as computed by the NOAA HYSPLIT model.

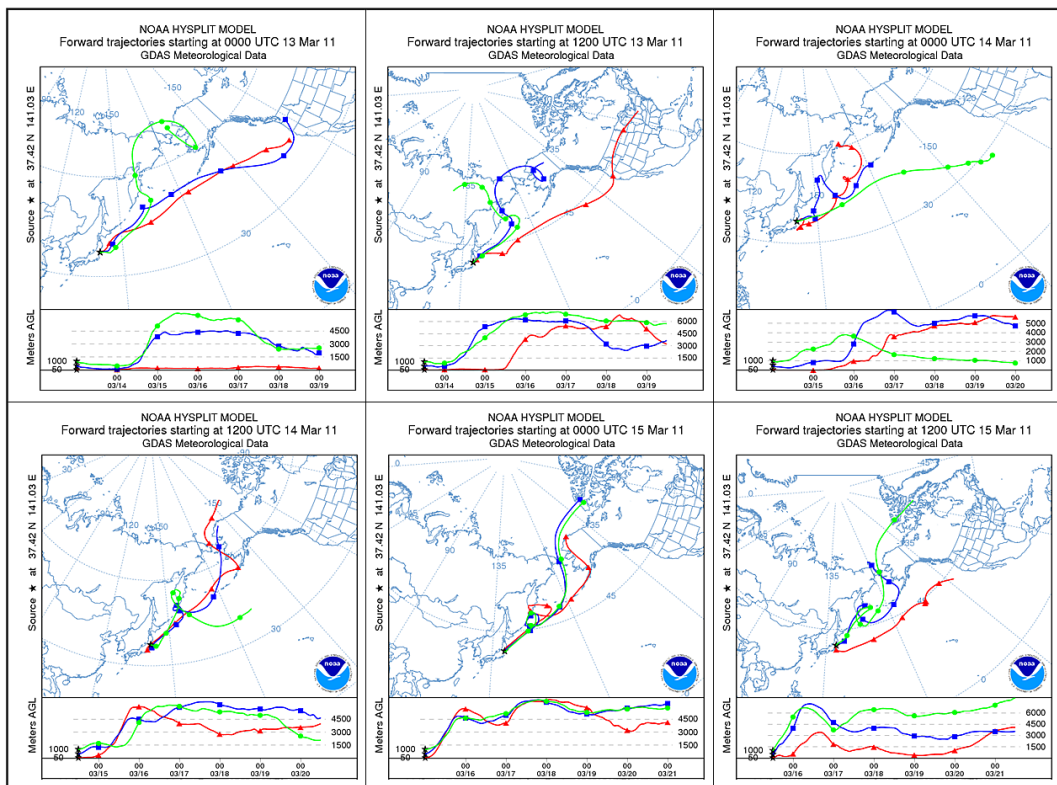


Figure 4 Trajectories of air masses released at heights of 50 m (red), 500 m (blue) and 1,000 m (green) from the Fukushima Daiichi nuclear power plant originating at 00 UTC and 12 UTC from 13 to 15 March 2011 as computed by the NOAA HYSPLIT model.



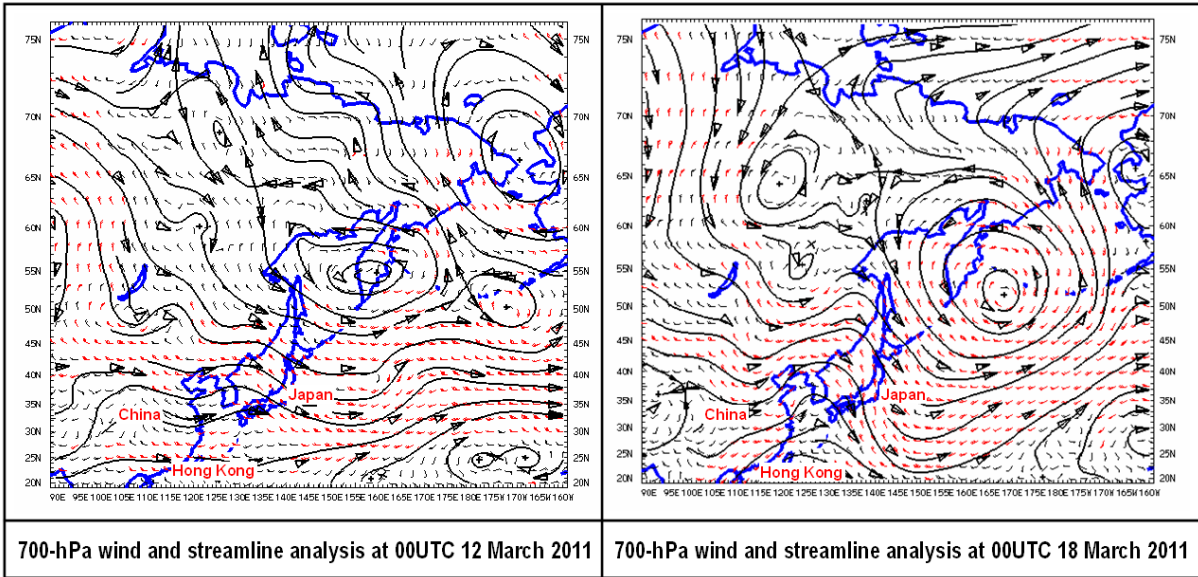


Figure 5(a) Intensification of a cyclonic system over the Bering Sea as depicted on the 700-hPa wind and streamline analysis charts on 12 and 18 March. Air masses were caught up by the cyclonic circulation and followed a looping motion in the vicinity of the Kamchatka Peninsula. (Source: Model analysis data from Japan Meteorological Agency)

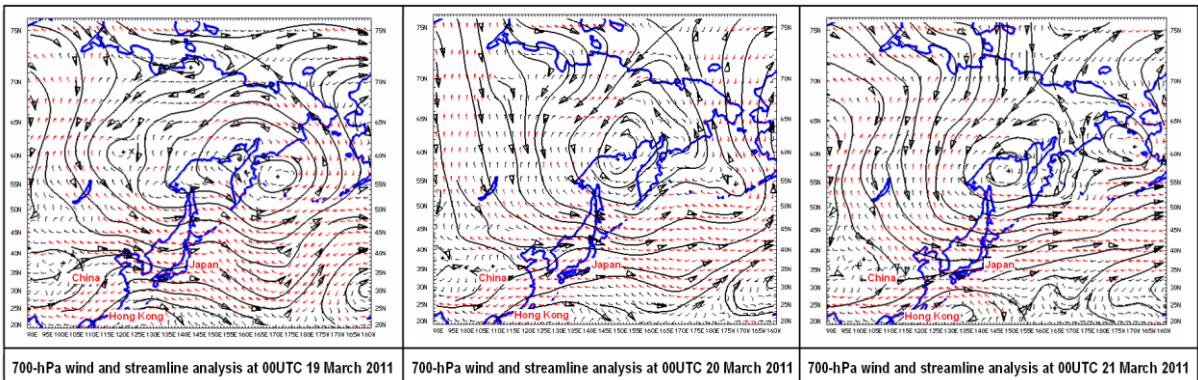


Figure 5(b) 700-hPa wind and streamline analysis charts from 19 to 21 March showed that the cyclonic circulation near the Kamchatka Peninsula drifted westwards and lingered over the sea area west of the Kamchatka Peninsula. Under the influence of the cyclonic flow, air masses moved in an anti-clockwise direction towards northeastern China. (Source: Model analysis data from Japan Meteorological Agency)

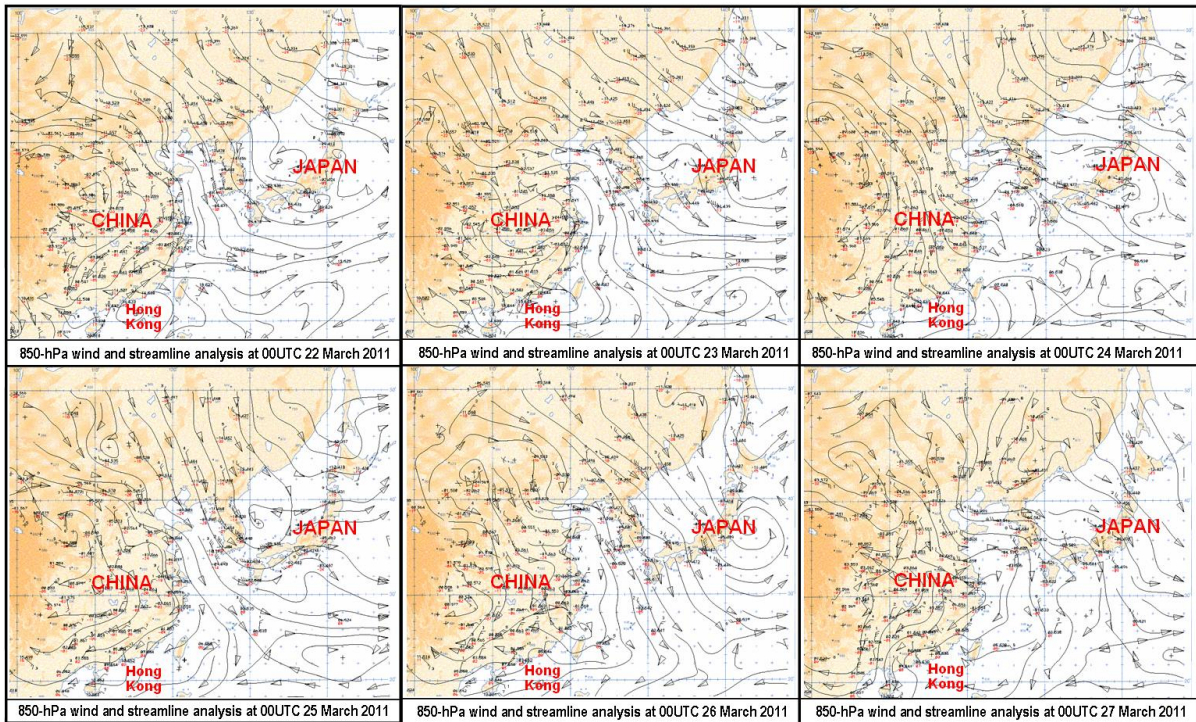


Figure 6 850-hPa wind and streamline analysis charts from 22 to 27 March 2011. Air masses over northeastern China were transported to the south by the north to northeasterly airstream. (Source: Model analysis data from Hong Kong Observatory)

As from Figure 5(b), significant north to northwesterlies originating from higher latitudes dominated over southeastern Russia and northeastern China on 21 March. The associated subsidence is expected to bring a downward vertical motion of air masses as they travelled. A lower level, say at 850-hPa corresponding roughly to an altitude of 1,500 m, becomes more representative in subsequent analysis.

As shown in the 850-hPa wind and streamline analysis charts from 22 to 27 March (Figure 6), a northerly airstream dominated over mainland China. A northeast monsoon prevailed over southern China at the surface level. Air masses over northeastern China are expected to move southwards under the northerly airstream.

Figure 7 shows the backward trajectory of air masses reaching Hong Kong at 18 UTC 26 March 2011 as computed by HYSPLIT. The trajectory is calculated for 72 hours backward in time. The result indicates that the air masses could be originated from northeastern China on around 24 March and travelled along the eastern coast of China as they descended from an altitude of about 1,500 m.

NOAA HYSPLIT MODEL  
 Backward trajectory ending at 1800 UTC 26 Mar 11  
 GDAS Meteorological Data

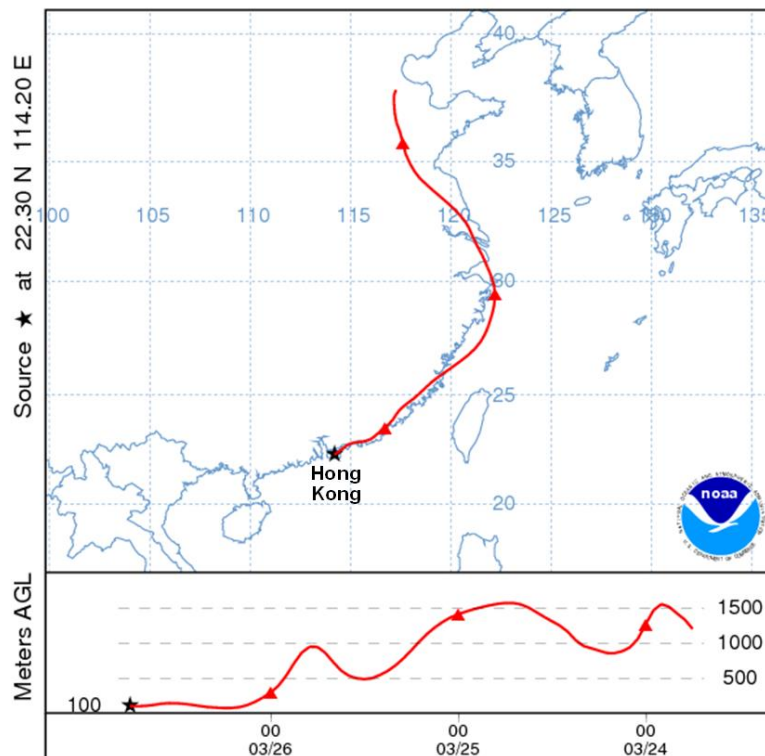


Figure 7 Backward trajectory of air masses reaching Hong Kong at 18 UTC 26 March 2011 as computed by the NOAA HYSPLIT model. The air masses originated from northeastern China on around 24 March at an altitude of about 1,500 m and travelled along the eastern coast of China in reaching Hong Kong.

Monitoring results from the Comprehensive Nuclear-Test-Ban Treaty Organization (CTBTO, 2011) confirmed that, at their station at Ussuriysk in Russia, near the China-Russia border east of Heilongjiang,  $^{131}\text{I}$  was first detected on 22 March. The dates of first detection of artificial radionuclides at various places over eastern Asia are shown in Figure 8. From airborne particulate samples in China,  $^{131}\text{I}$  was first detected at Heilongjiang and Beijing over the northeastern part of the country on 23 and 25 March respectively, at Zhejiang over the eastern coast on 26 March, and then at Hong Kong on 27 March. Time evolution of these monitoring results is in good agreement with the synoptic assessment that the air masses may have spread south along the eastern coast of China.

Based on these observations, it was postulated that the first batch of artificial radionuclides from Fukushima had likely followed a tortuous path across the eastern parts of Russia and China before reaching Hong Kong, as illustrated by the schematic diagram of probable trajectory in Figure 9. As the northeast monsoon persisted, artificial radionuclides were detected in six



consecutive daily samples from 27 March to 1 April (Table 1).

The northeast monsoon gradually weakened after 1 April. With the establishment of a low level anticyclone south of Japan, winds over the coast of southeastern China turned east to southeasterly (Figure 10). The change in wind direction could have made it less favourable for the dispersion of radioactive substances from mainland China. Between 3 and 5 April, light rain was recorded intermittently in various places over Hong Kong. Furthermore, as revealed from the synoptic meteorological observations, rain was also observed in the vicinity of Hong Kong. The rain might have some effect in washing down the aerosols and particulates in the atmosphere and therefore decreasing the concentration of airborne particulates. Figure 11 shows the time series of the maximum daily rainfall recorded over Hong Kong and the activity of  $^{131}\text{I}$  in daily airborne particulate samples collected at King's Park from 15 March to 31 April. The absence of artificial radionuclides in the samples collected from 2 to 5 April could be due to the change in wind direction over the coast of southeastern China together with the effect of rain in Hong Kong and its vicinity.

By the end of March, artificial radionuclides originating from Fukushima were detected all across the northern hemisphere by the CTBTO stations (CTBTO, 2011). Therefore, it became rather difficult to trace the pathway for the second batch of the artificial radionuclides detected in Hong Kong after 6 April. Hernández-Ceballos *et al.* (2012) indicated that it took less than 21 days to complete a revolution of the mid-latitude surface westerlies. The possibility of the artificial radionuclides taking an around-the-globe route before arriving Hong Kong in early April cannot be ruled out.



Figure 8 Dates of first detection of  $^{131}\text{I}$  from airborne particulates originating from the Fukushima nuclear accident as detected in various places over Asia. CTBTO monitoring stations are marked with red dots, while those operated by local authorities are marked in blue. The sampling period for monitoring stations in mainland China and Hong Kong was 24 hours, while that in Taiwan was a 7-day period from 22 to 28 March. (Sources: CTBTO; Radiation Monitoring Technical Centre, Hangzhou; and Taiwan Atomic Energy Council)

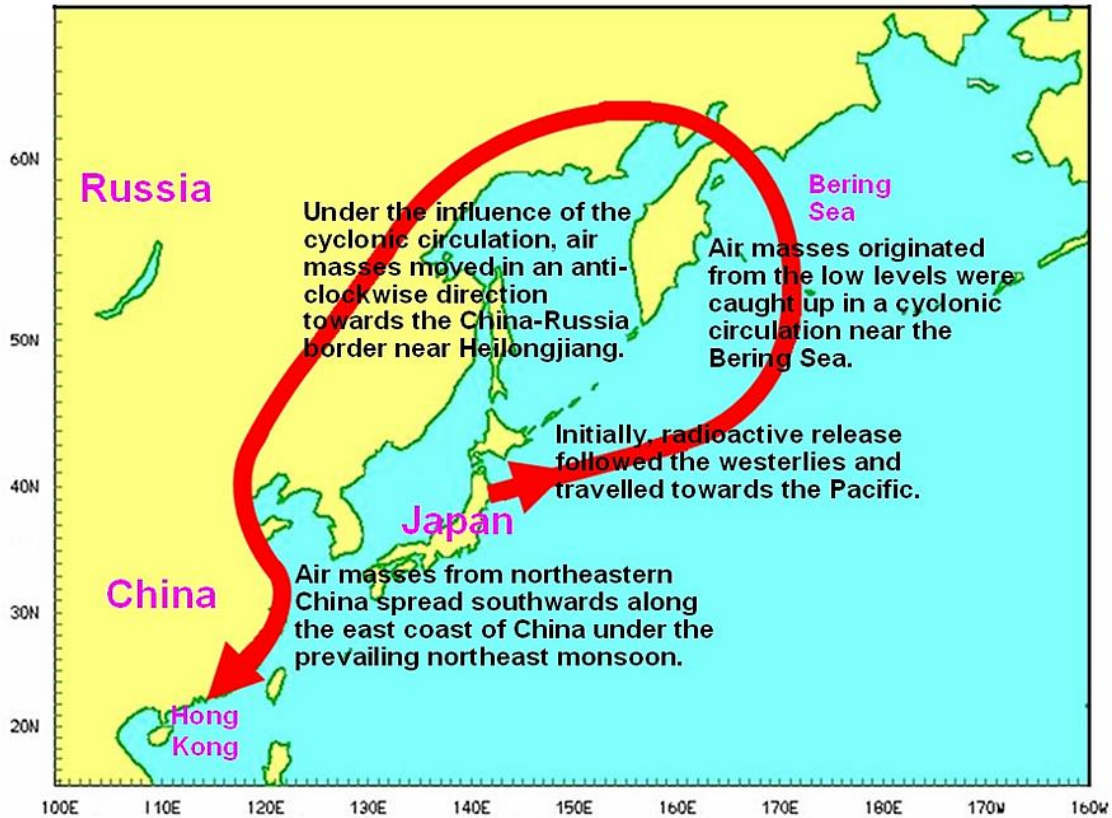


Figure 9 Schematic diagram showing the possible trajectory of the first batch of radioactive substances from Fukushima to Hong Kong.

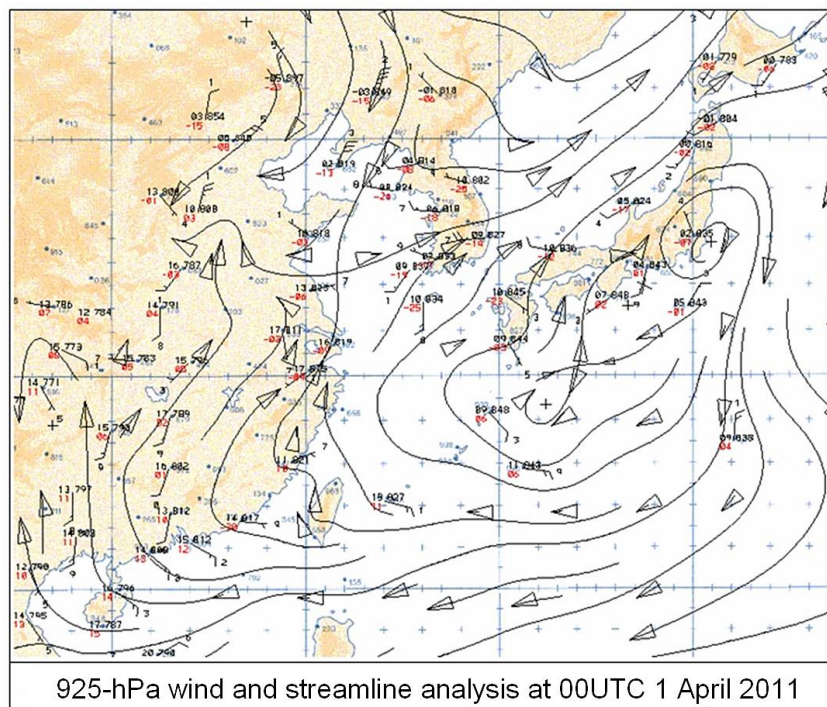


Figure 10 An anticyclone established over the sea south of Japan on 1 April 2011. Low level winds over the coast of southeastern China turned east to southeasterly. (Source: Model analysis data from Hong Kong Observatory)

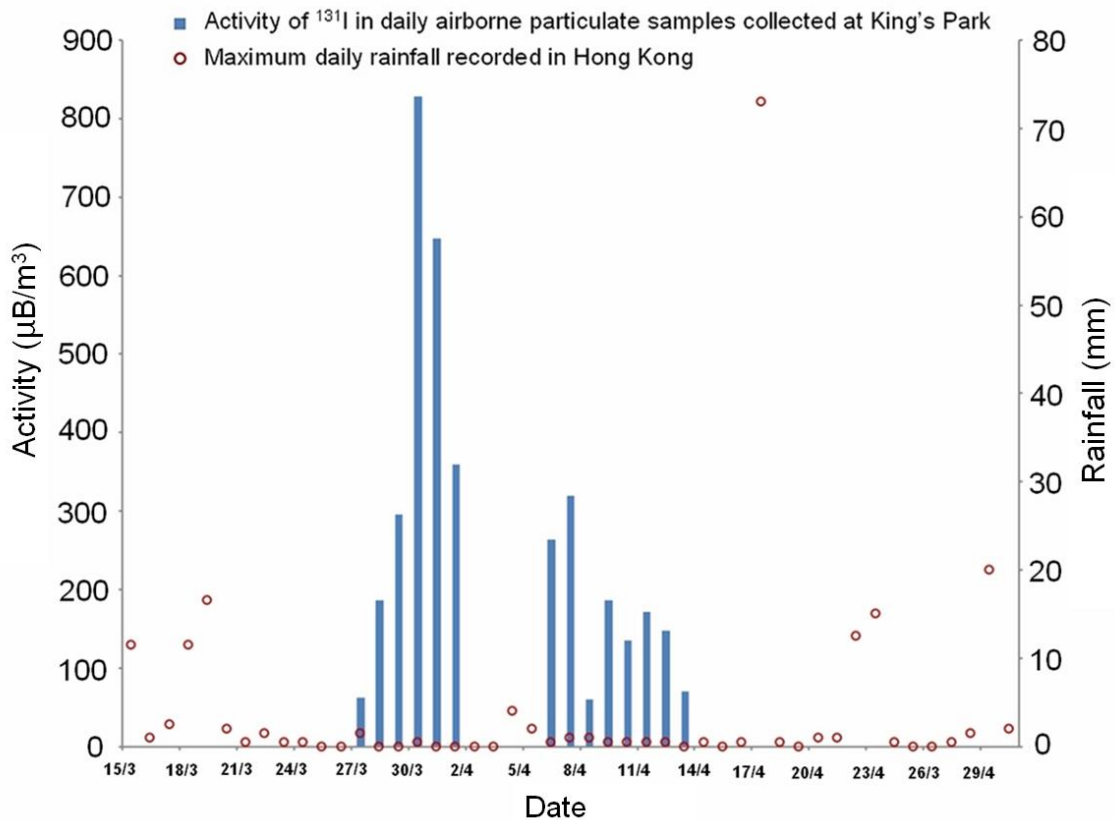


Figure 11 Activity of  $^{131}\text{I}$  in daily airborne particulate samples collected at King’s Park and daily maximum rainfall recorded in Hong Kong from 15 March to 30 April

### 3. Simulation Results using FLEXPART

To further assess the pathway of the first arrival of  $^{131}\text{I}$  in Hong Kong, a long range dispersion model is also employed to simulate the transportation of radioactive release from the Fukushima accident. Model simulation was carried out by using the Lagrangian particle dispersion model FLEXPART (Stohl *et al.*, 2005), which can handle multiple particles with diffusion, dry and wet deposition, as well as radioactive decay of the transported materials. The results presented below are based on the simulation with source term from Chino *et al.* (2011) and modified by Terada *et al.* (2012), together with global meteorological data, based on actual analysis by NCEP at  $0.5^\circ$  horizontal resolution and 3-hour temporal resolution. The model run initialized at 00 UTC on 11 March 2011, covers the period from 11 to 31 March 2011. Outputs include near-surface activity concentration and deposition.

Figure 12 shows the simulated activity concentration of  $^{131}\text{I}$  over eastern Asia and western north Pacific from 13 to 29 March 2011. It is noted that the dispersion pathways of the radionuclide are in general consistent with those



described in Section 2 above. Initially, the radioactive materials followed the westerlies and spread eastwards. Some of them were influenced by the cyclonic circulation over Bering Sea and turned in an anti-clockwise direction towards the China-Russia border near Heilongjiang. The radioactive materials then travelled southwards along the eastern coast of China and reached Hong Kong on 27 March.

From the simulation results, some radioactive materials over the western north Pacific were transported quickly towards the southwest and reached the Philippines on 23 March. This was consistent with the detection of artificial radionuclide by the CTBTO station at the Philippines on 23 March as shown in Figure 8.

Time series of the simulated  $^{131}\text{I}$  activity in Hong Kong at 12 UTC from 26 to 31 March is shown in Figure 13. The model result could rightly depict the rise in  $^{131}\text{I}$  activity after 26 March, although it under-estimated the values by about one order of magnitude.

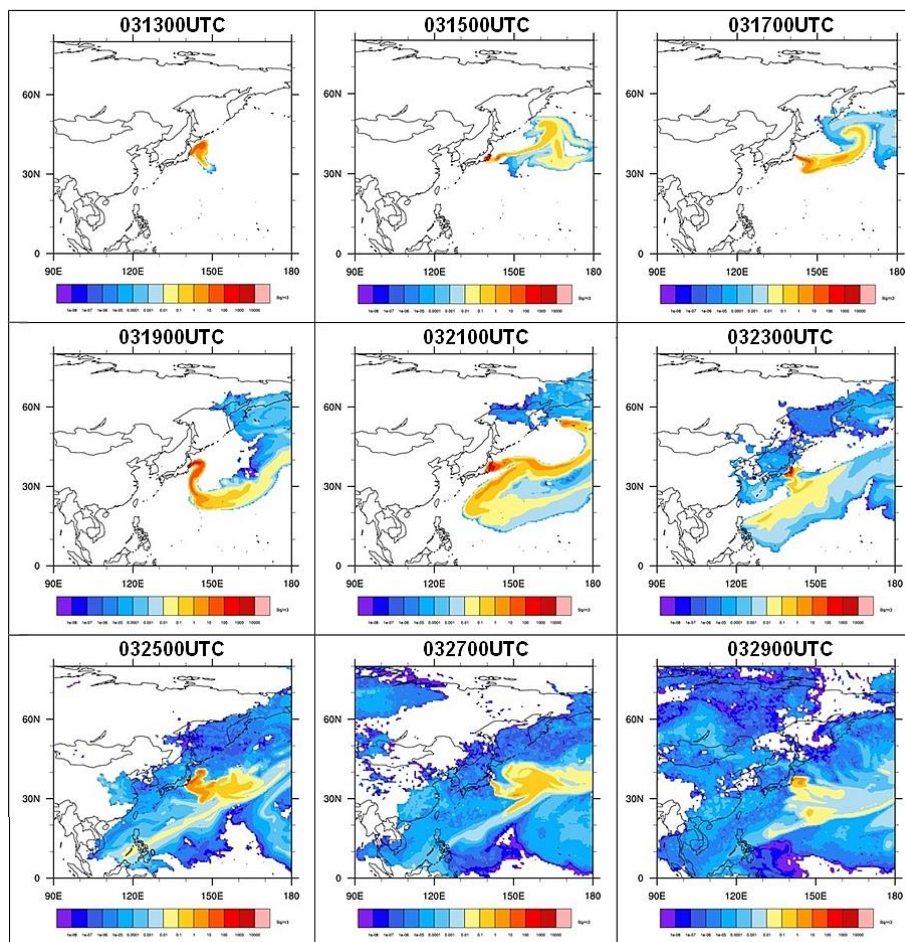


Figure 12 Distribution of activity concentration of  $^{131}\text{I}$  over the western north Pacific and eastern Asia from 13 to 29 March 2011.



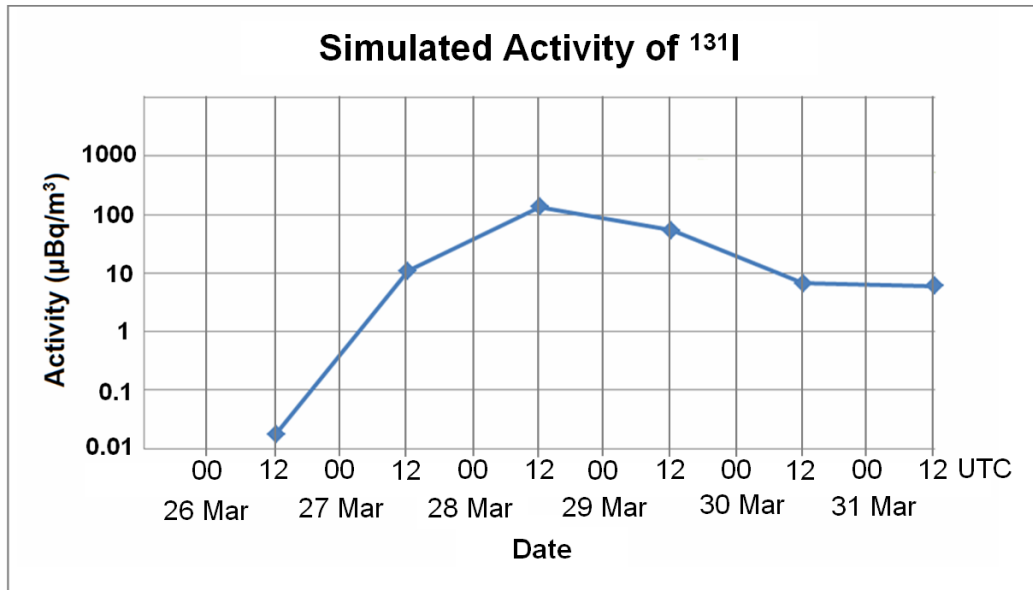


Figure 13 Simulated activity of <sup>131</sup>I in Hong Kong at 12 UTC from 26 to 31 March 2011

#### 4. Discussions and Conclusions

The probable pathway for radioactive materials transported from Fukushima to Hong Kong was examined. Based on an analysis of the synoptic meteorological conditions together with the use of HYSPLIT and various radiation monitoring results in the region, the assessment is that the first batch of radioactive materials might have taken a tortuous route through eastern Russia and mainland China before reaching Hong Kong. The above assessment is also compared favorably with the simulation results from FLEXPART in terms of the first arrival time in March 2011. For the second batch of artificial radionuclides, it became rather difficult to trace their origin. The possibility of the artificial radionuclides taking an around-the-globe route before arriving Hong Kong in early April cannot be ruled out.

The dispersion of radioactive substances from Fukushima was closely related to changes in the atmospheric conditions and synoptic patterns. Numerical tools such as HYSPLIT and FLEXPART proved very useful for assessing the spread of the plume arising from a point source and explaining the likely movement scenarios followed by the released radioactive substances.

However, as in the case of Fukushima, reliable source terms for assessing accident severity and consequences in real-time were not readily available in the early phase given the rather challenging circumstances. In fact, even in the post-analyses of source terms for the accident, results can still vary significantly due to different simulation techniques and weather prediction scenarios.

Therefore, the inherent uncertainty involved poses questions in the adequacy of an early assessment, not to mention that a whole range of simulation results are expected from different dispersion models. As such, the adoption of some kind of ensemble approach by taking various potential release situations into consideration for scenario assessment may be helpful, especially when an imminent off-site release is expected and yet the plant conditions remain unclear. For example, Draxler *et al.* (2013) used five different atmospheric transport and dispersion models to simulate the deposition and air concentration for the Fukushima accident and showed that the ensemble mean of a subset of better performing members could provide more consistent results. For better support of scenario forecasts, trajectory analyses and consequence assessment, it is also considered worthwhile to explore the possibility of having a suite of numerical models, deploying a multi-scale and multi-model system, including numerical weather prediction in the regional scale; and trajectory forecast for a fast and quick assessment, as well as more accurate atmospheric transport modelling (e.g. Stohl *et al.* 2011; Arnold *et al.* 2013) for flexible deployment and integrated implementation.

## References

Arnold, D., Seibert, P., Nagai, H., Wotawa, G., Skomorowski, P., Baumann-Stanzer, K., Polreich, E., Langer, M., Jones, A., Hort, M., Andronopoulos, S., Bartzis, J.G., Davakis, E., Kaufmann, P. and Vargas, A., 2013: Lagrangian Models for Nuclear Studies: Examples and Applications, in Lagrangian Modeling of the Atmosphere (eds. J. Lin, D. Brunner, C. Gerbig, A. Stohl, A. Luhar and P. Webley), American Geophysical Union.

Chino, M., H. Nakayama, H. Nagai, H. Terada, G. Katata, and H. Yamazawa, 2011: Preliminary Estimation of Release Amount of  $^{131}\text{I}$  and  $^{137}\text{Cs}$  Accidentally Discharged from the Fukushima Daiichi Nuclear Power Plant into the Atmosphere, *Journal of Nuclear Science and Technology*, 48 (7), 1129–1134.

CTBTO, 2011: Fukushima-related measurements by the CTBTO - radioactivity also measured in the southern hemisphere. Retrieved from <http://www.ctbto.org/press-centre/highlights/2011/fukushima-related-measurements-by-the-ctbto/>.

Draxler, R.R., and G.D. Hess, 1998: An overview of the HYSPLIT\_4 modeling system of trajectories, dispersion, and deposition. *Aust. Meteor. Mag.*, 47, 295-308.

Draxler, R., D. Arnold, S. Galmarini, M. Hort, A. Jones, S. Leadbetter, A. Malo, C. Maurer, G. Rolph, K. Saito, R. Servranckx, T. Shimbori, E. Solazzo and G. Wotawa, 2013: World Meteorological Organization's model simulations of the radionuclide dispersion and deposition from the Fukushima Daiichi nuclear power plant accident, *Journal of Environmental Radioactivity*. Retrieved from <http://dx.doi.org/10.1016/j.jenvrad.2013.09.014>.

Draxler, R.R. and Rolph, G.D., 2014: HYSPLIT (HYbrid Single-Particle Lagrangian Integrated Trajectory) Model access via NOAA ARL READY Website (<http://ready.arl.noaa.gov/HYSPLIT.php>). NOAA Air Resources Laboratory, Silver Spring, MD.

Hernández-Ceballos, M.A., G.H. Hong, R.L. Lozano, Y.I. Kim, H.M. Lee, S.H. Kim, S.-W. Yeh, J.P. Bolívar, M. Baskaran, 2012: Tracking the complete revolution of surface westerlies over Northern Hemisphere using radionuclides emitted from Fukushima, *Science of The Total Environment*, Volume 438, 1 November 2012, pages 80-85.

Hong Kong Observatory, 1992: Environmental Radiation Monitoring in Hong Kong, Technical Report No. 8, Background Radiation Monitoring Programme 1987-1991, Hong Kong Observatory. Retrieved from <http://www.hko.gov.hk/publica/rm/rm008.pdf>

Hong Kong Observatory, 1997: Environmental Radiation Monitoring in Hong Kong, Technical Report No. 15, Annual Report 1996. Hong Kong Observatory. Retrieved from <http://www.hko.gov.hk/publica/rm/rm015.pdf>.

IAEA, 2011: “IAEA International Fact Finding Expert Mission of the Fukushima Dai-ichi NPP Accident Following the Great East Japan Earthquake and Tsunami,” International Atomic Energy Agency, 2011. Retrieved from [www-pub.iaea.org/MTCD/meetings/PDFplus/2011/cn200/documentation/cn200\\_Final-Fukushima-Mission\\_Report.pdf](http://www-pub.iaea.org/MTCD/meetings/PDFplus/2011/cn200/documentation/cn200_Final-Fukushima-Mission_Report.pdf).

Lee, B.Y. and K.C. Tsui, 1991: Retrospective Analysis of Radiation Fallout in Hong Kong after the Chernobyl Accident in 1986, Environmental Radiation Monitoring in Hong Kong, Technical Report No. 6, Hong Kong Observatory.

Lee, Olivia S.M., C.M. Lui, C.H. Yung, 2012: Summary of Environmental Radiation Monitoring in Hong Kong 2011, Technical Report No. 32, Hong Kong Observatory.

Leon, J. Diaz, D.A. Jaffe, J. Kaspar, A. Knecht, M.L. Miller, R.G.H. Robertson, A.G. Schubert, 2011: Arrival time and magnitude of airborne fission products from the Fukushima, Japan, reactor incident as measured in Seattle, WA, USA. *Journal of Environmental Radioactivity*, 102 (2011) 1024-1031.

Masson, O., A. Baeza, J. Bieringer, K. Brudecki, S. Bucci, M. Cappai, F.P. Carvalho, O. Connan, C. Cosma, A. Dalheimer, D. Didier, G. Depuydt, L.E. De Geer, A. De Vismes, L. Gini, F. Groppi, K. Gudnason, R. Gurriaran, D. Hainz, Ó. Halldórsson, D. Hammond, O. Hanley, K. Holeý, Zs. Homoki, A. Ioannidou, K. Isajenko, M. Jankovic, C. Katzlberger, M. Kettunen, R. Kierepko, R. Kontro, P.J.M. Kwakman, M. Lecomte, L.L. Vintro, A.-P. Leppänen, B. Lind, G. Lujanienė, P.M. Ginnity, C.M. Mahon, H. Malá, S. Manenti, M. Manolopoulou, A. Mattila, A. Mairing, J.W. Mietelski, B. Møller, S. Nielsen, J. Nikolic, R.M.W. Overwater, S.E. Pálsson, C. Papastefanou, I. Penev, M.K. Pham, P.P. Povinec, H. Ramebäck, M.C. Reis, W. Ringer, A. Rodriguez, P. Rulík, P.R.J. Saey, V. Samsonov, C. Schlosser, G. Sgorbati, B.V. Silobritiene, C. Söderström, R. Sogni, L. Solier, M. Sonck, G. Steinhauser, T. Steinkopff, P. Steinmann, S. Stoulos, I.

Sýkora, D. Todorovic, N. Tooloutalaie, L. Tositti, J. Tschiersch, A. Ugron, E. Vagena, A. Vargas, H. Wershofen, O. Zhukova, 2011: Tracking of airborne radionuclides from the damaged Fukushima Dai-Ichi nuclear reactors by European networks. *Environ. Sci. Technol.* 2011, 45 (18), 7670–7677.

National Diet of Japan, 2012: Executive Summary of the Official Report by the Fukushima Nuclear Accident Independent Investigation Commission, The National Diet of Japan.

Stohl, A., C. Forster, A. Frank, P. Seibert, and G. Wotawa, 2005: “Technical Note: The Lagrangian Particle Dispersion Model FLEXPART Version 6.2”, *Atmospheric Chemistry and Physics*, 5 (9), 2461-2474

Stohl, A., P. Seibert, G. Wotawa, D. Arnold, J. F. Burkhart, S. Eckhardt, C. Tapia, A. Vargas, and T. J. Yasunari, 2011: Xenon-133 and caesium-137 releases into the atmosphere from the Fukushima Dai-ichi nuclear power plant, determination of the source term, atmospheric dispersion, and deposition. *Atmospheric Chemistry and Physics*, 2011, 11:28319-28394.

Terada, H, G. Katata, M. Chino, H. Nagai, 2012: Atmospheric discharge and dispersion of radionuclides during the Fukushima Dai-ichi Nuclear Power Plant accident. Part II: verification of the source term and analysis of regional-scale atmospheric dispersion, *Journal of Environmental Radioactivity*, 112, 141-154.